

UNIVERSITY OF CALIFORNIA

Santa Barbara

Compact Phase Shifter Design Using Barium Strontium Titanate
Thin-Film Varactors

A Thesis submitted in partial satisfaction of the
requirements for the degree of Master of Science
in Electrical and Computer Engineering

by

Justin Lee Serraiocco

Committee in charge:

Professor Robert A. York, Chair

Professor Umesh K. Mishra

Professor James S. Speck

September 2003

The thesis of Justin Lee Serraiocco is approved.

James S. Speck

Umesh K. Mishra

Robert A. York, Committee Chair

August 2003

ABSTRACT

Compact Phase Shifter Design Using Barium Strontium Titanate Thin-Film Varactors

by

Justin Lee Serraiocco

Phase shifters are important components in many microwave subsystems used for radar and communication. Current technology makes phase shifters very costly, and inhibits widespread adoption of devices such as phased-array antennas. Barium strontium titanate (BST) thin-film varactor technology enables the creation of low cost analog phase shifters. Research is presented here that describes how to further decrease the cost of BST phase shifter modules by use of lumped element inductors and high impedance transmission lines. Most notably, a X-band reflection-type phase shifter using BST varactors achieved 250° of phase shift while measuring only 0.36mm^2 .

Contents

1	Introduction	1
1.1	Analog versus Digital	2
1.2	Current Phase Shifter Technology	3
1.3	New Phase Shifter Technologies	4
1.3.1	MEMS	4
1.3.2	RF CMOS	5
1.3.3	LTCC	6
1.3.4	Integrated BST passives	6
2	Integration of Passives and BST Thin-films	8
2.1	Component Modeling	9
2.2	Process Flow	11
3	Reflection-Type Phase Shifters	15
3.1	Distributed versus Lumped	16
3.2	Resonator Loads	18
3.3	Quadrature Hybrid Couplers	19
3.4	X-band BST RTPS Designs	21
3.4.1	Lange coupler based	21
3.4.2	Lumped coupler based	23
3.4.3	Impedance transformed couplers	27

4	Distributed Analog Phase Shifters	34
4.1	Strategies for Size Reduction	38
4.2	Synthetic Transmission Lines	39
4.3	High Impedance Coplanar Strip Transmission Lines	45
4.4	Comparisons	51
5	Conclusion	55

Chapter 1

Introduction

Phase shifter circuits are found in microwave systems such as phased-array antennas and highly linear power amplifiers. In a phased-array antenna system, phase shifters are used to electrically control the output beam direction. In power amplifiers, phase shifting feedback networks are used to compensate for AM-PM distortion and other nonlinearities. Without phase shifters, an electrically scanned array antenna could not be built; a physically rotating directional antenna would have to be used. Enhanced efficiency power amplifiers can be built without phase shifters, but might have to use techniques such as baseband predistortion, which require more hardware support. The phase shifter is a crucial device for realizing these two types of circuits, and many others.

One might be led to believe from the above description that the phase shifter is a device complicated in operation and design. However, quite the opposite is true. The phase shifter is a two-port device, whose sole responsibility is alter an input signal's relative phase according to a control signal. Ideally, this task would be accomplished with no attenuation. The design of the phase shifter can be as simple as connecting four quarter-wave transmission lines with a pair of varactor diodes. However, more efficient designs require a bit more thought.

1.1 Analog versus Digital

One of the primary characteristics of a phase shifter is the nature of its control signal. Analog phase shifters have a single analog input control voltage, giving infinite resolution theoretically. Digital phase shifters have n digital input signals offering a resolution limited by the least significant bit. For a 4-bit digital phase shifter, this is typically 22.5° . Both types have their advantages and drawbacks, and are suited for different purposes.

Digital phase shifters require switches capable of passing microwave signals to function. The switches can be realized electromechanically, or with solid-state technology such as pin diodes or FETs. Obtaining higher phase shift resolution with digital phase shifters generally requires the addition of more control bits. As is the case with all digital circuits, they are generally less sensitive to power supply and temperature variations than their analog counterparts.

Most analog phase shifters rely on a voltage variable capacitance, or varactor, to function. Varactors also can be implemented electromechanically, with diodes, or with ferroelectric films. Using a single analog control voltage, it is possible to obtain very precise phase shifts. Unlike digital designs, analog designs are very sensitive to process variations and their operating environment.

Analog phase shifters are a natural fit for linearized power amplifiers. The error detection circuits in feedforward and feedback amplifiers output analog signals. These voltages can be sent directly to an analog phase shifter, which corrects the input or output signal. Using a digital phase shifter here would require adding an analog to digital converter. The limited resolution of most digital phase shifters also makes them a poor fit for linearization circuitry.

Phased-array antenna systems are usually computer controlled, and hence

output digital control signals. When analog phase shifters are used, each must be paired with a digital to analog converter. Digital phase shifters do not require this additional circuitry, and may be more suitable for array purposes. A few other considerations must be taken into account when deciding the more appropriate phase shifter type. For example, the single control voltage of the analog phase shifter reduces the wiring complexity on the surface of the array compared to a digital implementation.

1.2 Current Phase Shifter Technology

Traditionally, phase shifters for phased-array antenna systems have been implemented with ferrites. These devices have evolved over the last few decades to become smaller, less lossy, and more power efficient. There are a variety of different designs offering high performance, but all share a common drawback. In order to tune the ferrite material, strong magnetic fields must be generated. This is most commonly done with coils requiring bias voltages in the hundreds to thousands of volts. Ferrite phase shifters are also very slow, requiring long tuning times. Most ferrite phase shifter designs are not amenable to mass production methods, which keep their unit costs very high. Phased-arrays implemented with ferrite phase shifters are not cost-effective for terrestrial commercial applications.

The maturation of GaAs MESFET technology over the last decade has made feasible the creation of all solid-state phased-arrays. GaAs MMIC technology offers the broadest range of options for the creation of phase shifter circuits. Both varactors and switches are available, enabling analog and digital designs. Both distributed and lumped components are available as well. The only drawback of MMIC technology is cost. In the past, with the military as their only customer, MMIC designers have not been very sensitive to cost considerations. With the recent explosion in commercial

and consumer wireless products, more cost effective phase shifter designs have begun to emerge. The increased market for MMIC devices has also reduced fabrication costs.

1.3 New Phase Shifter Technologies

Even though GaAs MMIC technology continues to mature, with yields and wafer diameters increasing continuously, they are still a costly option for the microwave design engineer. Several research technologies are receiving attention as potential candidates to supply phase shifters for cost sensitive markets. Most of these technologies can be applied to reduce the costs of other types of microwave circuits as well. Most of these technologies are capable of reducing the cost of microwave phase shifters to a fraction of their current prices, and some can offer higher performance as well.

1.3.1 MEMS

MEMS (micro-electro-mechanical systems) technology uses advanced thin-film processing techniques to realize miniaturized mechanical systems. Both switches and varactors can be realized using multiple metal layers and carefully controlled etchings. The process flow usually involves temperatures below 200°C , and is therefore compatible with standard semiconductor processing. This potentially allows integration with GaAs MMIC or CMOS technologies. The advantages of MEMS for phase shifters is low loss and low parasitics. MEMS switches are capable of routing very high frequency microwave signals with very little loss. MEMS varactors use air or vacuum as their dielectric, and have negligible leakage as a result. Carefully designed devices can function up to 100 GHz, rivaling the best semiconductor technologies. These attributes make MEMS technology attractive for low loss and high frequency applications.

A drawback of MEMS technology for phase shifter implementation is the large number of processing steps. Since it uses the standard lithographic tools of the semiconductor industry, the costs are similar. A MEMS switch process can exceed fifteen mask layers, making processing costs high. An additional problem with MEMS technology is packaging. The thin metal membranes functioning as switching elements or varactors are very sensitive to their environment, and must be packaged in either an inert or vacuum environment. Hermetic packaging increases cost and makes the device more bulky. It also reduces the potential for integration with other circuit components. Another drawback are the large control voltages required. Reduction of these voltages results in increased phase noise and device fragility. Typical voltages for robust operation are in the range of 80 to 100 volts.

1.3.2 RF CMOS

A decade ago, the use of CMOS technology for microwave circuits would have been considered unthinkable. However, the continual scaling of CMOS transistors to smaller dimensions and higher frequencies have made CMOS a viable technology for microwave circuits. A number of variations on the CMOS process, including BiCMOS using silicon-germanium HBTs and silicon on insulator technology, extend the power and frequency handling capabilities of CMOS even higher. With huge investments in technology and infrastructure from the digital IC business, CMOS can be an attractive proposition for high volume microwave and mixed-signal integrated circuits. However, the high costs of prototyping circuits in leading-edge CMOS technology makes development costs very high. The necessity of 'first-time-right' design, driven principally by high masks costs, increases development time and makes design revisions very costly. For low and moderate volume applications, RF CMOS may not be feasible.

1.3.3 LTCC

Low temperature cofired ceramic technology uses multiple layers of insulating ceramics together with metallic pastes to realize microwave circuits. It allows a three-dimensional integration aspect not feasible with thin-film multilayer technologies. The metallic pastes can be high conductivity, for realizing transmission lines, inductors, and capacitor plates, or low conductivity, for integrated resistors. Different types of ceramics can also be integrated together. Higher dielectric constant thin layers for realizing capacitors, or low dielectric constant thick layers to reduce parasitic coupling. More recently, the integration of ferroelectric, piezoelectric, and ferrite ceramic layers has been accomplished. This allows the creation of tunable microwave components, such as phase shifters, directly within the LTCC structure. More conventionally, it is also possible to integrate semiconductor components on the surface or within a cavity of the LTCC stack. The integration of arbitrary types of transistors and diodes for gain, switching, and tuning makes LTCC technology very flexible. LTCC technology uses lower resolution lithography than is necessary for MEMS or CMOS technologies. Overall, LTCC technology seems very promising for realizing low cost and highly integrated microwave circuits. The technology is relatively new, and is just beginning to reach widespread usage.

1.3.4 Integrated BST passives

The technology explored in this thesis is the integration of barium strontium titanate (BST) with traditional thin-film passive technology. The passives are implemented with conventional semiconductor processing techniques on dielectric substrates. Processing thin-film passives is less costly than MMIC and CMOS processes, since the tolerances are greater and the substrates are cheaper. Resistors, capacitors, inductors, and transmission lines can

be integrated onto a substrate in a simple process. When these passives are integrated with flip-chip or wirebonded active components, the resulting device is sometimes referred to as a multi-chip-module (MCM). This process is capable of creating high performing, compact circuits. Circuit sizes and external component counts need to be kept to a minimum to ensure economic feasibility. The addition of a thin-film varactor technology to a passives process can help achieve this. By integrating varactors, only gain and switch stages need to be added as discrete devices to complete the functionality a module. Analog phase shifters can be created without using any external components. Extremely low cost phase shifters can then be realized with proper circuit design to minimize circuit size. Some of the designs explored here can also be implemented in other technologies, but the low cost nature of the integrated BST process may make it the most appropriate for realizing low cost microwave phase shifters circuits.

Chapter 2

Integration of Passives and BST Thin-films

The goal of integrating passive thin-film components with a BST varactor is to allow the development of extremely low-cost tunable microwave components. At lower microwave frequencies, distributed circuit design techniques cannot be used because they result in uneconomically large circuit sizes. Lumped element design must be scaled up in frequency to function at frequencies up to around 10 GHz. The integration of a low cost, high performing varactor with spiral inductors, transmission lines, capacitors, and resistors is key to this effort.

Current varactor circuit elements vary in loss and tunability. Hyper-abrupt pn junction diodes can have tuning ratios in excess to 10:1, but can become very lossy with tuning. MEMS varactors have typical tunabilities of less than 1.5:1, but with extremely low loss, even deep into the millimeter-wave region. To maintain reasonable losses with a moderate Q technology at typical microwave frequencies, a tuning ratio of at least 2:1 is essential. Lower tuning ratios greatly increase the difficulty of realizing design objectives, necessitating the cascade of multiple stages. This increases the overall circuit size and reduces performance.

The BST material was grown on c-plane sapphire substrates using rf

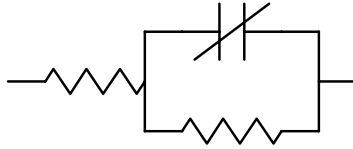


Figure 2.1: The BST varactor circuit model.

magnetron sputtering. The initial setup and materials costs for a sputtering system are much lower than those of other deposition technologies, such as MOCVD or MBE. The films were sputtered from multiple ceramic targets consisting of varying ratios of barium and strontium. A 50:50 ratio would give films of higher tunability, but a 30:70 film would have less loss, and a higher breakdown voltage. Application of a dc bias voltage to the capacitor alters the dielectric constant, resulting in a capacitance change. Initial design optimistically assumed a 3:1 tuning ratio. Later designs assumed a more realistic 2.5:1 or 2:1 ratio.

2.1 Component Modeling

The BST deposition system was used primarily for material science research, and consistency was difficult to obtain. Variations in the dielectric constant, tuning range, and loss were encountered from growth to growth. It was difficult to take into account all of these variations in a design. Constructing an accurate model of the BST varactor posed a serious challenge. The basic circuit model is shown in figure 2.1. The series resistor represents electrode loss, and the parallel RC circuit represents the capacitance and the dielectric loss.

Attempting to characterize the electrode losses in the parallel plate varactor structure proved very difficult. The thin metal layers and small dimen-

sions rendered standard treatments of the ohmic loss inaccurate. Extraction of data directly from test structures was attempted. Data accurate enough for use in models was difficult to obtain due to measurement uncertainty and variations in individual devices. Attempts to extract the dependence of electrode loss on parameters such as length, width, and gap through a comprehensive set of test structures failed. It was difficult to correlate the extracted values with the simple three element circuit model. The varactor structure was also simulated in a full wave finite element electromagnetic simulator. It again proved difficult to extract circuit model data from the simulations. However, a correlation was made between higher Q and a wider, shorter capacitor structure. This went against the previously held belief that a long, skinny electrode was better. Both EM simulations and fabricated device measurements indicated that a wider structure had less ohmic loss.

Assigning a value to the capacitor in the circuit model was a simple matter. Obtaining the correct capacitance in the fabricated circuit proved to be more difficult. Initially, no fringing capacitance was assumed to be present. Later, analysis indicated that there was approximately a twenty percent increase in capacitance due to fringing. This fringing capacitance reduces the tunability of the varactor, and it is desirable to minimize it. For a given area, the shape with the smallest periphery is a square. Since fringing is proportional to periphery, the square is the ideal capacitor shape. Using formulas adapted from [?], a synthesis procedure was developed to obtain the desired zero bias capacitance using a square capacitor.

Dielectric loss measurements are a simple matter at 100 MHz, but are considerably more complicated at 10 GHz. The test structures accommodating the varactor and the high frequency coplanar probe made extracting accurate data difficult. Measurement of a small capacitor at high microwave frequencies stressed the accuracy of the test equipment. An additional complication

was variation of the loss with bias. There was no attempt made to account for this variation.

The inaccuracy of closed form spiral inductor models is well known. An addition complication beyond modeling the inductive and resistive contribution is modeling the coplanar capacitive components. Most published works assume an ground beneath the substrate, and use the simple parallel plate capacitance formula. There is only a single treatment of coplanar ground capacitance [?]. Even that is only a simplistic model, approximating the spiral traces and grounds as asymmetric coplanar strip transmission lines. Using electromagnetic simulation to account for finite metal thickness increased simulation times ten fold.

2.2 Process Flow

The lengthy high temperature BST sputter deposition process dictated that the initial step in the process had to be the fabrication of the varactor structure. This is beneficial because it allows the optimal processing of the varactor without regard to damage to other circuit components. However, the ferroelectric material is itself very sensitive to the subsequent processing steps. Oxygen plasma cleaning, for example, could significantly change the dielectric constant of the deposited material. The sensitivity of BST to hydrogen gas meant that PECVD deposition of silicon nitride was not an option. The oxygen plasma cleaning was kept to a minimum, but was sometimes inevitable when lithographic mistakes were made. The restriction on PECVD prevented a quick and easy method to passivate the varactors.

The first step in processing the BST varactors was deposition of the bottom electrode. As mentioned previously, only electrode materials capable of withstanding the high growth temperatures could be considered. Unfortunately this rules out most high conductivity metals, leaving platinum as the

best option. After depositing a thin layer of titanium for adhesion, $200nm$ of platinum was deposited via e-beam. The restriction on the thickness of this layer came from the structure of the overlay BST capacitor. The dielectric layer needs to be thicker than the bottom electrode to prevent a short circuit when the top electrode was deposited. The BST layer was limited to approximately $300nm$, since growth times longer than three hours excessively degraded the films. This thickness resulted in a relative dielectric constant of approximately 450, giving a capacitance density of $15fF/\mu m^2$. This density was about the highest that could be tolerated, given the operating frequencies chosen, and the contact lithography methods used. Platinum is not easily etched, so a liftoff technique was used.

After growth in the sputtering system, the BST was wet etched in a solution of hydrofluoric acid. Different samples had vastly different etch rates and uniformity. Depending on the condition of the growth chamber, a tough interfacial layer could be formed at the bottom electrode. This layer often proven impossible to etch through, necessitating that the process be started again from scratch.

Normally, the top electrode was deposited at this stage. However, when high valued biasing resistors were integrated into the process, it was necessary to deposit it first. A $40nm$ thick layer of nichrome was used as the resistor material. This material's resistivity is not that large, and the $5k\Omega$ resistors needed had to be made very narrow and meandered to meet both the resistivity and size requirements. The deposition of a thick top electrode prior to resistor deposition prevents high resolution contact lithography due to planarity issues. Therefore, the nichrome material deposited via e-beam first. The thinness of this layer did not interfere with the resolution of the top electrode layer. The composition of this electrode varied, but usually consisted of a $100nm$ platinum layer capped with a $500nm$ gold layer, both

deposited via e-beam and lifted-off.

Once the varactors and resistors were fabricated, two thick gold layers were deposited for the coplanar transmission lines, interconnects, spiral inductors, and air-bridges. The first gold layer measured one micron thick, and was the primary trace layer. Then, a thick resist impervious to normal solvents was deposited for the air-bridge support. A second one micron gold layer was then deposited to form the bridge. To create thicker gold spirals without developing complicated liftoff stacks, backside lithography, or electroplating, the second gold layer was sometimes selectively layered onto the base spiral inductor metalization, doubling the thickness in most places. A gap was kept between the air-bridges and this thicker layer to prevent shorting. The fabricated circuits were tested using on-wafer coplanar probes and a network analyzer. For further details on the BST overlay varactor device and process, consult [1].

Bibliography

- [1] B. Acikel, "High Performance Barium Strontium Titante Varactor Technology for Low Cost Circuit Applications," Ph.D thesis, University of California, Santa Barbara, 2002

Chapter 3

Reflection-Type Phase Shifters

The reflection-type phase shifter (RTPS) is simple phase shifter design that uses a minimal number of components. It is most commonly realized in analog form, with a single input control voltage. The RTPS can be realized in many different forms, but all include a quadrature coupler and dual, identical reflective loads. The reflective loads are one-port circuits with variable phase reflection characteristics. The quadrature coupler's function is to isolate the input and output signals, turning the phase shifting behavior of the reflective load into more usable two-port device.

The reflective load responsible for the phase shift can be realized in many different ways. The simplest is to use a tunable shunt capacitor. Realizing larger amounts of phase shift requires resonating the capacitor with an inductor or quarter-wave transmission line section. The technique most appropriate depends on the technology used to implement the phase shifter. Variables such as loss and size must also be taken into account when deciding on a reflective load topology.

Equal in importance to the reflective load is the circuit which separates the input signal from the reflected output signal. The ideal circuit would contain three ports, one each for the input signal, reflection load, and output signal, and have appropriate isolation between the ports. Such a device,

called a circulator, requires the use of bulk ferrite materials and is not easily integrated into a microwave IC. A workable alternative is to use a four-port device. A reciprocal four-port circuit with the appropriate isolation properties can be realized in thin-film form, and is termed a quadrature hybrid coupler. The coupler divides an input signal from any port into the two opposite ports, while isolating the adjacent one. In order to obtain the expected behavior, two reflection loads must be included in the RTPS, connected to the coupled and thru ports of the hybrid. The RTPS's phase shifted input signal is found at the hybrid's isolated port, and will ideally be isolated from the RTPS input signal.

Proper selection of the form for the quadrature coupler and reflection load is critical to obtaining the most effective RTPS design. Variables such as operating frequency, cost, and size will determine the appropriate circuits in any given process technology.

3.1 Distributed versus Lumped

When monolithic technology is used to realize a circuit, an important consideration is minimization of die area. This can make the use of transmission line components a costly proposition. At frequencies above 20 GHz, distributed components shrink to acceptably small sizes. The combination of moderately high dielectric constants ($\epsilon_r > 10$), wafer thinning, and thru-wafer vias make microstrip transmission lines at high frequencies relatively compact. Therefore, reflective load designs utilizing transmission lines are an option in MMIC processes at high frequencies.

If thru-wafer vias are not available, uniplanar transmission lines such as coplanar waveguide can be used. However, the effective dielectric constant of a CPW transmission line is approximately $(\epsilon_r + 1)/2$, leading to transmission line lengths nearly twice that of electrically equivalent microstrip lines. CPW

transmission lines are more costly in terms of die area than microstrip transmission lines on identical substrates. Techniques exist for reducing transmission line sections to shorter lengths. In [1], reduced length transmission lines were realized using high impedances lines with shunt capacitors. This technique produces transmission lines that appear nearly identical to those using full length transmission lines, but only over a narrow bandwidth.

At lower microwave frequencies, even reduced length transmission line components become very long, and lead to unreasonably large dies if used. The use of integrated thin-film lumped components, such as spiral inductors and metal-insulator-metal (MIM) capacitors, becomes necessary to achieve smaller die areas. This requires the addition of air-bridge and dielectric deposition steps to a simple passive circuits process. These additional processing steps increase processing complexity and reduce yield, increasing costs. The payoff is greater flexibility in circuit design.

A concern with lumped thin-film components is maintaining a high quality factor, or Q . Distributed circuit components are usually assumed to have Q of 200. Lumped components can be substantially lower. One of the main concerns is maximizing spiral inductor Q . The insulating nature of typical microwave IC substrates eliminates many causes of low Q in found in silicon processes, but getting large Q s can still be a challenge. The principle method of raising Q s is to use thick metalization layers, with high conductivity metals such as copper. The skin and current crowding effects [?] limit the effectiveness of using very thick metal layers. Poor closed-form models for planar spiral inductors further increase the challenge of realizing high Q . Optimization via electromagnetic simulation is a must for maximizing inductor quality factors.

3.2 Resonator Loads

Much of the literature on reflection-type phase shifter reflective loads focuses on distributed approaches using high tunability varactor diodes. This makes it a challenge to discern whether an approach is feasible for compact realization with limited tuning BST varactor.

The simplest reflective load is a single shunt capacitor. This approach can be highly effective when the phase shift necessary is not large, or hyper-abrupt tuning diodes are available. In [2], equation (3.1), was given to describe the phase shift behavior of a such a reflective load. r_C represents the tuning ratio of an ideally selected varactor, and is greater than one.

$$\Delta\phi = 2(\arctan(\sqrt{r_C}) - \arctan(\frac{1}{\sqrt{r_C}})) \quad (3.1)$$

Most MMIC varactors are limited to an r_C of around four, and a corresponding phase shift range of about 70° . For BST technology with a tuning range of about 2:1, this reduces to 40° . The phase shift range required for almost any application is usually greater than 90° . Only varactor diodes with special doping profiles are usually able to achieve large tuning ranges. However, most of these devices have low Q. Therefore, the single varactor technique is not that useful except in limited circumstances where loss is not a huge concern or the required phase shift is small.

In [3], a technique is described for adding the admittances of two diodes to double the phase shift. This was accomplished by using a $\lambda/4$ transmission line of an appropriate impedance. In [4], a reflective load consisting of two separate varactor circuits resonating at different frequencies was used to extend the phase shift range of low tuning varactors. Both of these techniques are effective at increasing the phase shift range of a reflective load, but are not appropriate for realizing compact phase shifters. The former

technique introduces a bulky quarter-wave transmission line, which is still of significant size even when implemented with reduced-length high impedance capacitively loaded lines. The latter technique uses two separate resonant circuits, which will result in a large amount of insertion loss variation over bias when implemented with components of low to moderate Q.

The only technique suitable for use in compact reflection-type phase shifter circuits is the LC reflective load. Here, the variable capacitance of the varactor is resonated with a series inductor. The appropriate design equations are given in [2].

$$\Delta\phi = 4 \arctan\left(\frac{Z_{Cv0}}{Z_0} \frac{1}{2} \left(\sqrt{r_C} - \frac{1}{\sqrt{r_C}}\right)\right) \quad (3.2)$$

$$Z_{Cv0} = \frac{1}{\omega_0 C_{v0}} \quad (3.3)$$

$$L_l = \frac{Z_{Cv0}}{2\omega_0} \left(\sqrt{r_C} + \frac{1}{\sqrt{r_C}}\right) \quad (3.4)$$

Equation (3.2) gives the maximum differential phase shift when a varactor of center value C_{v0} is connected in series with an inductor of value L_l , as given by equation (3.4). This can increase the phase shift of limited tuning varactors to useful values. Notice, however, that when r_C is small, large inductances and small varactor capacitances result. This places an upper limit on the useful increase in phase shift possible with this technique.

3.3 Quadrature Hybrid Couplers

The function of the quadrature hybrid coupler in the reflection-type phase shifter is to separate the input and reflected signal of the reflective load. Network theory considerations dictate that a four port hybrid that splits the input signal into two output ports, isolates the fourth port, and is reciprocal, will have outputs in quadrature. This is not a concern for the RTPS, since

the phase difference is compensated for on the return trip through the hybrid towards the output port.

A variety of designs for the quadrature hybrid coupler are possible. The most basic is the branch-line hybrid [5]. This hybrid consists of four quarter-wave transmission lines connected end to end in a loop. The transmission lines are of different impedances, so that the thru and coupled ports remain impedance matched to the input. The input signal splits in quadrature between the thru and coupled ports, is bounced off the reflective loads, and recombines in phase at the isolated, or output port. This design is simple to realize in microstrip form. In coplanar waveguide, airbridges are required at the T-junctions to suppress moding. A total 12 air-bridges are required. The use of quarter-wave lines is of concern for monolithic implementations below 20 GHz. The size reduction techniques of [1] can be used if high quality shunt MIM capacitor are available. Even with heaving loading, the size of this hybrid is considerable.

Taking the size reduction technique of [1] to its maximum, and using a transmission line of infinite impedance transforms the transmission line into a pure inductance. The pi-network approximation of a transmission line is well known, and is used often to replace quarter-wave lines. The transformation of the branch-line hybrid from distributed to lumped form is generalized in [6]. A simplified version of the transformation equations is given in [2]. The most common lumped hybrid converts the four transmission line sections into two inductors and six capacitors. This conversion is the most popular because it minimizes the number of area consuming, and lossy, spiral inductors. Use of the generalized equations in [6] allows an impedance transformation from the input and output ports to the thru and coupled ports. This will allow enhanced phase shift performance to be achieved, as explained later.

A third quadrature hybrid coupler is the Lange coupler [7]. Consisting of

four or more tightly coupled transmission lines, the Lange coupler exhibits much wider bandwidth than branch-line or lumped couplers. It is also a quarter wavelength long, but is very narrow in the other dimension. This allows the Lange coupler to be bent in half, and reduced in length. The Lange coupler is very popular in MMIC design even at lower frequencies, because of its wide bandwidth and low loss. Its design more complicated than either the branch-line or lumped couplers.

3.4 X-band BST RTPS Designs

A number of different reflection-type phase shifter designs were implemented in the BST thin-film varactor process. A Lange coupler based design using an LC reflective load was designed first. Although the Lange coupler is long, its wide bandwidth allowed reasonable phase shifter performance to be obtained even if the center frequency of the reflective load was miscalculated. This could occur if either the inductor or BST dielectric constant was off in value. Designs using only lumped elements were also fabricated. Although not completely optimized in performance, these designs show promise for their extremely compact size. All circuits were designed to operate at a center frequency of 10 GHz.

3.4.1 Lange coupler based

The reflective loads for the Lange coupler based phase shifter was designed according to the equations described above. The LC reflective load was designed for a 180° phase shift at 10 GHz with a capacitance tuning ratio of 3:1. This resulted in a $1.6nH$ inductor and a $0.32pF$ zero bias varactor. This inductance is near the upper limit of achievable values at 10 GHz, due to self-resonant effects from capacitive parasitics. Its spiral had 2.5 turns, with an outer diameter of $300\mu m$, a conductor width of $25\mu m$, and a conductor

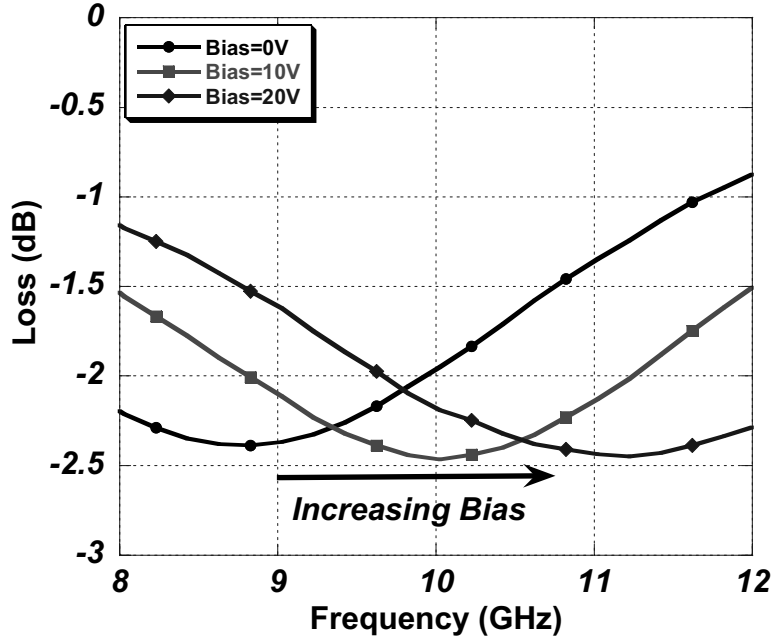


Figure 3.1: Phase shift performance of X-band LC reflective load.

spacing of $12\mu m$. The BST varactor dimensions were $4\mu m$ by $4\mu m$.

The actual phase shift achieved with this load was only 100° at 10 GHz. Further investigation revealed that the film capacitance density was approximately $9fF/\mu m^2$ instead of the desired $15fF/\mu m^2$. In addition, the film tunability was somewhat lower than the designed for 3:1 ratio. The reflective load exhibited a loss of -2.5dB at resonance, as seen in figure 3.1. This was larger than expected, but good enough to obtain promising results when integrated with the Lange coupler.

The Lange coupler was realized in a coplanar waveguide environment. Its center frequency was 10 GHz, giving it a length of $3300\mu m$ and an overall width of $650\mu m$. The thru and coupled ports of the Lange coupler were connected to a pair of the series LC resonators described above to complete the phase shifter. The circuit is pictured in figure 3.2.

The Lange reflection phase shifter gave a maximum of 120° phase shift

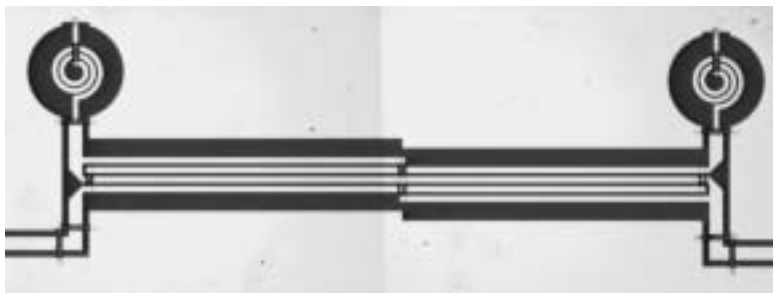


Figure 3.2: The completed BST reflection phase shifter using a Lange coupler.

near 11 GHz. At this frequency, it had less than $-3.3dB$ insertion loss for all biasing conditions. For the 10 GHz to 12 GHz frequency range, it was capable of over 100° phase shift with less than $-4dB$ insertion loss. Over the 8 GHz to 12 GHz range it maintained greater than $-15dB$ return loss. The complete performance data are given in figures 3.3 and 3.4.

3.4.2 Lumped coupler based

Large valued spiral inductors have significant parasitics that give them low self-resonant frequencies. The large dielectric constant of ferroelectric material results in high capacitance densities, which in turn results in small electrode areas. These two factors limit the achievable phase shift of a LC series resonator using a low tunability varactor. The approach suggested here is to utilize the degree of freedom given in equation (3.2) in choosing the characteristic impedance. By choosing a smaller Z_0 , a smaller inductance and a larger varactor capacitance result for a given phase shift. Smaller inductances have fewer parasitics and higher self-resonant frequencies. The inductors are also more compact. Due to the high dielectric constant of thin-film BST, increased capacitance actually eases layout and makes the stray parasitic capacitances less significant. The increase in electrode area is insignificant compared to the scale of the overall circuit. Normally, changing

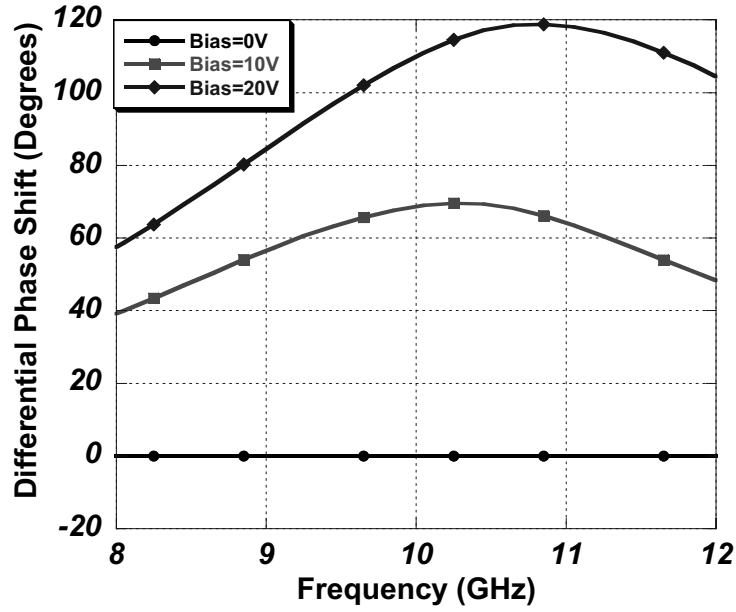


Figure 3.3: The Lange coupler RTPS differential phase shift over frequency.

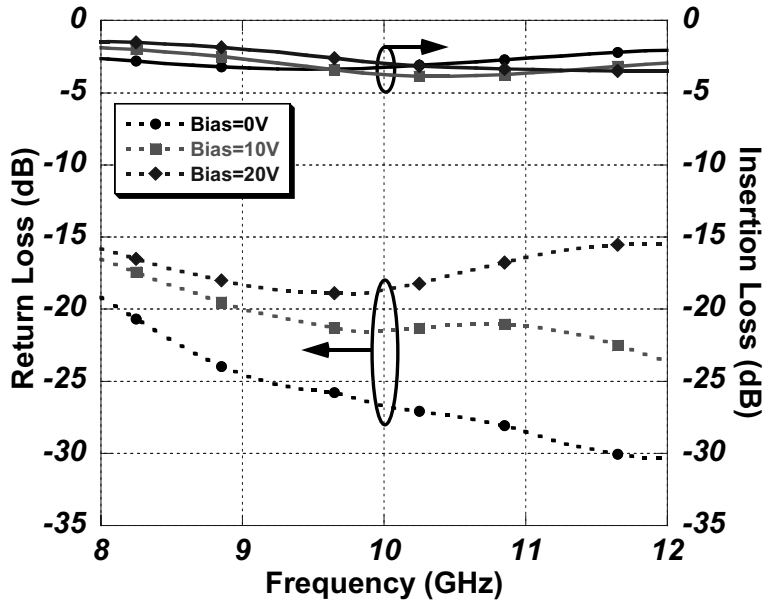


Figure 3.4: The Lange coupler RTPS insertion loss and return loss over frequency.

the characteristic impedance of a circuit is not a feasible design approach. However, the reflection loads are connected to the external world through a hybrid coupler. It is possible to maintain the input and isolated/output ports of the hybrid at the standard characteristic impedance of the external circuit while varying impedance of the thru and coupled ones [6].

The combination of a lumped element hybrid coupler and a lumped series LC resonator load can give phase shifters that consume very little substrate area, as first demonstrated in [2]. The design can potentially be extended to higher frequencies ranges and larger phase shifts by varying the characteristic impedance of the circuitry internal to the device. The approach also allows technologies with limited varactor tunabilities to achieve larger phase shifts than would be possible with a fixed impedance design.

Two lumped element reflection phase shifters were designed and tested. The first used a standard lumped element hybrid coupler with all ports having 50Ω output impedances. The hybrid's block diagram is given in figure 3.5, and consists of two $0.56nH$ inductors, two $0.32pF$ series capacitors, and four $0.13pF$ capacitors to ground. The hybrid is pictured together with its phase shifting load network in figure 3.6. As can be seen, the capacitors to ground were realized with two series capacitors of twice the design value. The original values were too small to realized reliably with contact lithography.

The LC resonator network consisted of a $1nH$ inductor and a varactor with $0.38pF$ zero bias capacitance. This would result in a 90° phase shift with 2:1 tuning. An identical circuit using only a shunt capacitor would exhibit 40° of phase shift. The circuit, complete with hybrid coupler, measured $900\mu m$ by $600\mu m$. Unlike the previous circuit, this one utilized square spiral inductors to minimize wasted space between circuit elements. At 10.5 GHz, the circuit had 105° of phase shift and a maximum of $-3.4dB$ of insertion loss. The performance is very narrowband and can be seen from the plots

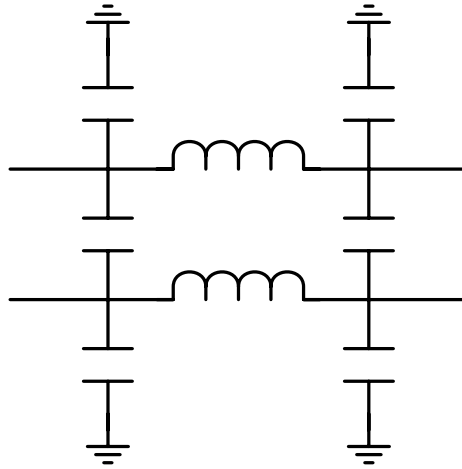


Figure 3.5: Circuit model of a conventional lumped element hybrid coupler.

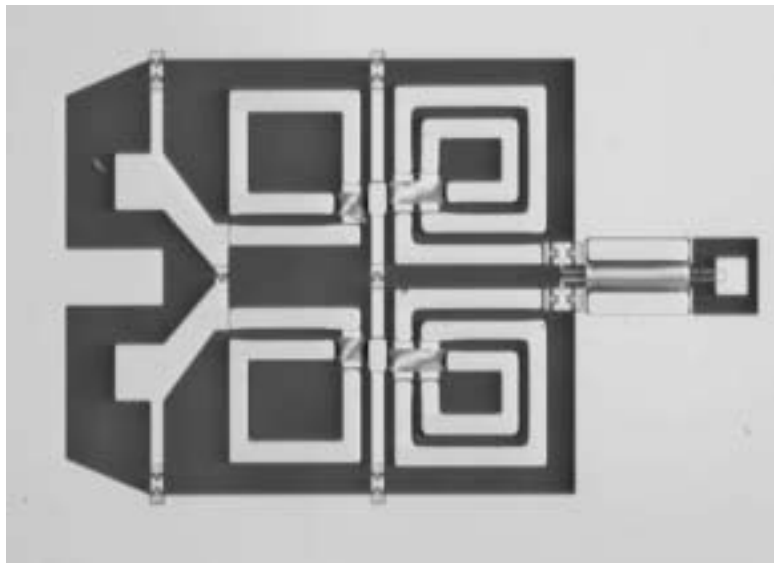


Figure 3.6: The completed lumped element reflection phase shifter measuring a scant $0.5mm^2$.

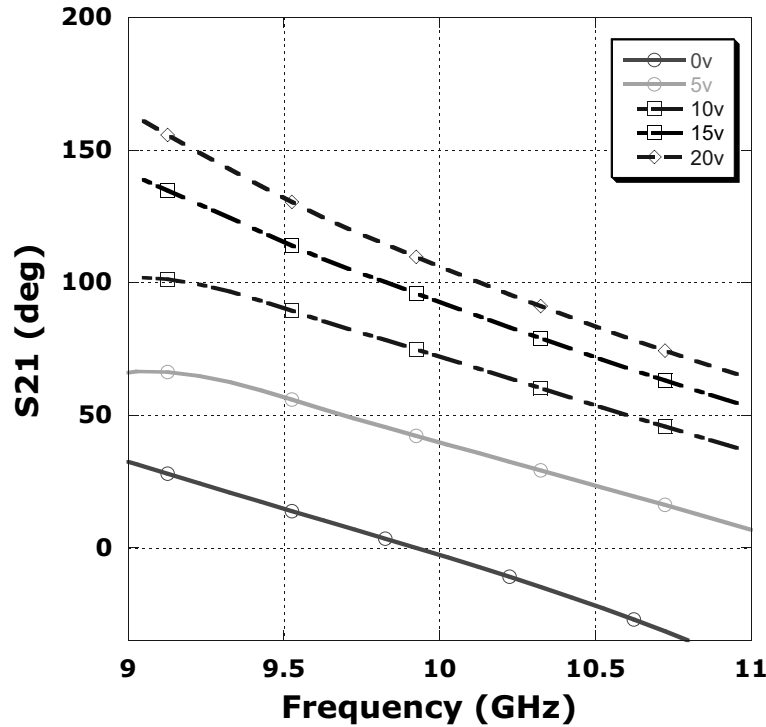


Figure 3.7: The lumped element RTPS differential phase shift over frequency.

in figures 3.7 and 3.8. This $30^\circ/dB$ is a significant improvement over first generation designs, and can be attributed to better modeling of the spiral inductors.

3.4.3 Impedance transformed couplers

If the characteristic impedance presented to the reflective loads is reduced, the achievable phase shift range can be increased. Since Z_0 is a parameter that impacts the entire system, it is necessary to use a transformer so that only the reflective loads have to be altered. A quarter-wave transformer is not a viable option for a compact circuit. If one was attached the lumped coupler described previously, it would increase the size of the circuit by many times. An lumped element LC transformer is a possibility, but would increase

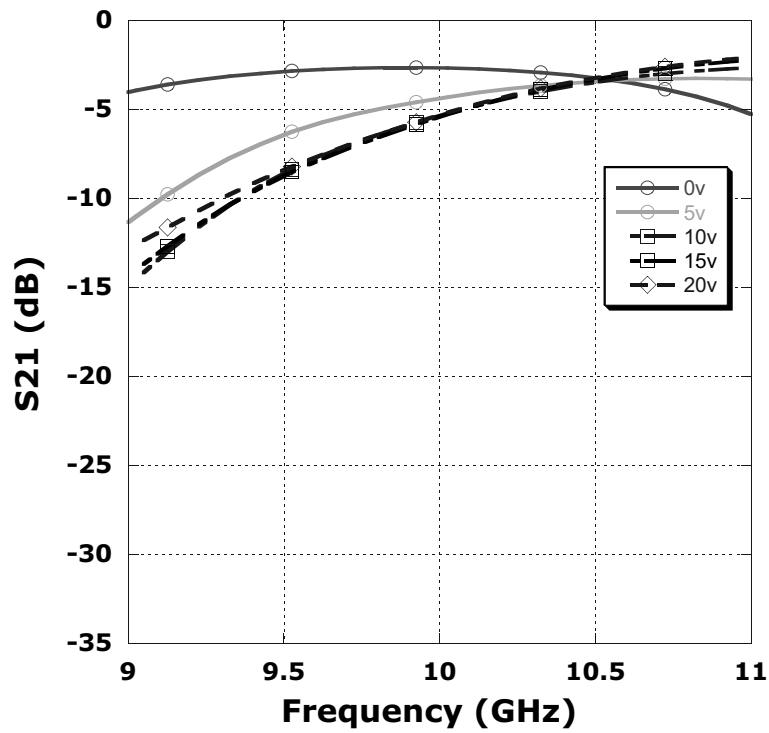


Figure 3.8: Insertion loss of the lumped element RTPS. The bandwidth is only a few hundred megahertz.

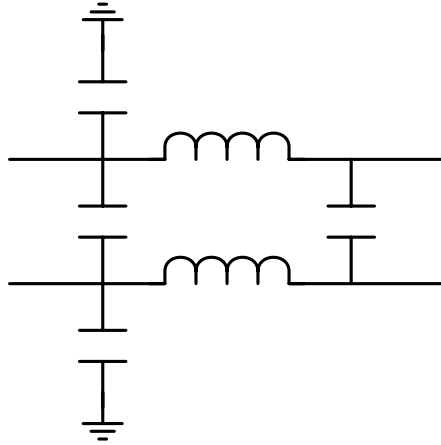


Figure 3.9: The impedance transforming lumped element hybrid coupler. The ports without shunt capacitors are reduced in impedance by one half.

circuit size and introduce additional loss. The solution previously proposed is to integrate the transforming behavior into the coupler, as described in [6]. The circuit model of the transforming coupler implemented is shown in figure 3.9.

The 10 GHz coupler design for the this second lumped element RTPS had two $0.4nH$ inductors, one $0.64pF$ capacitor, and three $0.32pF$ capacitors. The external input impedance of the coupler was 50Ω , but the reflective load ports had a characteristic impedance of 25Ω . With this lower impedance, higher amounts of phase shift are possible using smaller inductors and larger varactors, which are more easily implemented. Using a $1.4nH$ inductor, the circuit pictured in figure 3.10 achieved 250° of phase shift at 10.5 GHz. The circuit measures $600\mu m$ by $600\mu m$, for a total of $0.36mm^2$ of die area.

While a large amount of phase shift was achieved, the insertion loss was quite large. Figure 3.11 shows a wide band phase shift response, but figure 3.12 shows a maximum insertion loss of $-10dB$ at $10.5GHz$. Aside from the usual concerns due to inductor and BST varactor Q, the reduced impedance

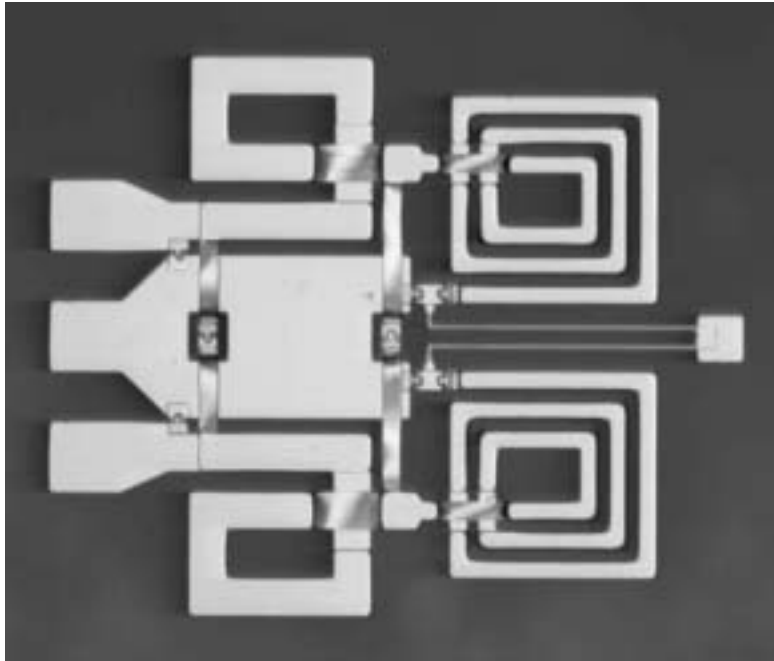


Figure 3.10: The reduced impedance RTPS. The circuit ground was moved to the center of the circuit to further reduce circuit size.

magnifies losses over what would be experienced with identical components in a 50Ω system. The lower impedance increases the currents flowing in the resonator through Ohm's law. Larger voltage drops are experienced across the parasitic resistances, increasing losses. The technique still holds merit though since, large phase shifts are simply not attainable from an LC reflective load with limited varactor tuning in a 50Ω system. For example, in a 50Ω system with 2:1 tuning, the inductor would have to be $4.6nH$ to achieve 250° of phase shift. Even if loss were not a concern, the parasitic capacitance of this component would cause it to resonate near 10 GHz.

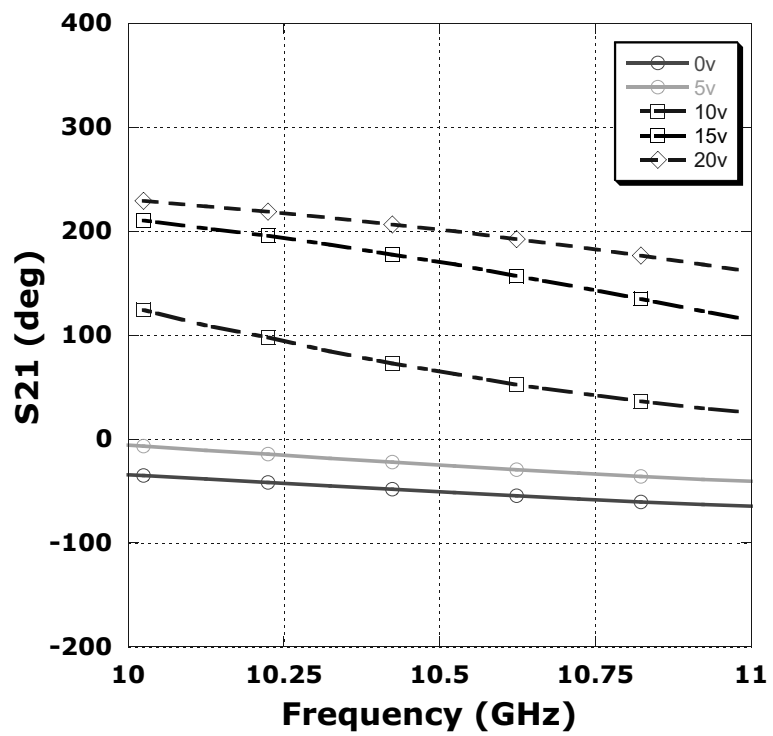


Figure 3.11: Phase shift performance of the reduced impedance RTPS.

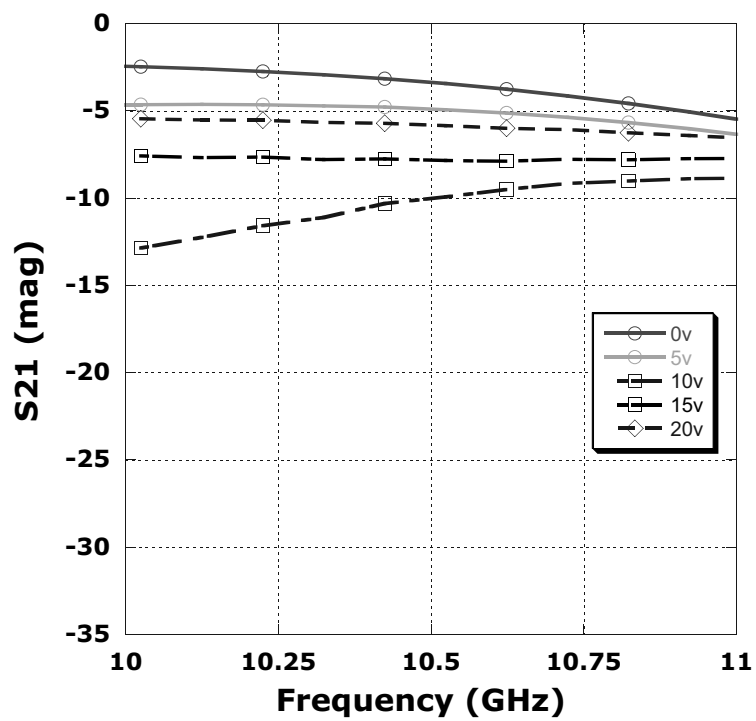


Figure 3.12: Insertion loss of the reduced impedance RTPS.

Bibliography

- [1] T. Hirota, A. Minakawa, and M. Muraguchi, "Reduced-Size Branch-line and Rat-Race Hybrids for Uniplanar MMIC's," *IEEE Trans. Microwave Theory Tech.*, vol.38, no.3, pp. 270-275, March 1990
- [2] F. Ellinger, R. Vogt, and W. Bachtold, "Compact Reflective-Type Phase-Shifter MMIC for C-Band Using a Lumped-Element Coupler," *IEEE Trans. Microwave Theory Tech.*, vol.49, no.5, pp. 913-917, May 2001
- [3] R.V. Garner, "360° Varactor Linear Phase Modulator," *IEEE Trans. Microwave Theory Tech.*, vol. 17, no.3, pp. 137-147, March 1969
- [4] D.M. Krafscik, S.A. Tmhoff, D.E. Dawson, and A.L. Conti, "A Dual-Varactor, Analog Phase Shifter Operating from 6 to 18 GHz," *IEEE 1988 Microwave and Millimeter-Wave Monolithic Circuits Symposium*, pp. 83-88
- [5] D.M. Pozar, *Microwave Engineering*, Wiley, New York, 1998
- [6] R.W. Vogel, "Analysis and Design of Lumped and Lumped-Distributed Element Directional Couplers for MIC and MMIC Applications," *IEEE Trans. Microwave Theory Tech.*, vol.40, no.2, pp. 253-262, Feb. 1992
- [7] J. Lange, "Interdigitated Stripline Quadrature Coupler," *IEEE Trans. Microwave Theory Tech.*, vol.17, pp. 1150-1151, Dec. 1969

Chapter 4

Distributed Analog Phase Shifters

The distributed analog phase shifter is attractive for its simple fabrication and wide bandwidth. The device is realized by periodically loading a high impedance transmission line with variable shunt capacitance. This results in a transmission line with a tunable electrical length. There has been great interest in the design recently, because of its compatibility with ferroelectric and MEMS varactor technologies. The often understated drawback of the distributed phase shifter is its long length. Devices operating around 10 GHz usually have lengths measured in centimeters. The low tuning ratio of MEMS varactors results in a transmission line length several times that of semiconductor or ferroelectric based designs. The long length makes semiconductor based distributed phase shifters impractical for cost sensitive applications. The lower fabrication costs of the alternative technologies make the distributed phase shifter design more practical for low cost applications, but reductions in length can further decrease costs and improve yields.

A distributed phase shifter is created by adding tunable capacitance to a transmission line. Adjusting the capacitance alters the phase velocity of the signal propagating along the line, varying its electrical length, and therefore the phase shift. Altering the capacitance also changes the characteristic

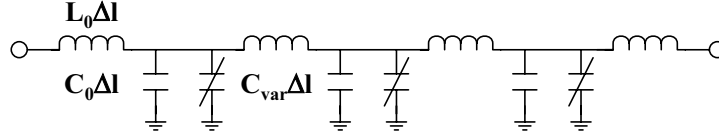


Figure 4.1: Circuit approximation of a distributed analog phase shifter.

impedance of the transmission line, so an impedance mismatch can occur as the circuit is tuned. Theoretically, it should be possible to add both series and shunt tunable reactance to the transmission line to keep an impedance match with tuning; however, a technology for adding tunable series inductance has yet to be fully developed. Ferroelectric varactors, MEMS bridges and switches, and semiconductor diodes are all capable of adding capacitance. In the majority of cases, the shunt capacitance is added periodically as discrete elements to the transmission line. This capacitance loading makes the distributed phase shifter a periodic structure, with a passband and a stopband. Careful design is necessary to ensure the frequencies of interest fall into the passband, while simultaneously maintaining a high performing, efficient structure.

A simple circuit model for the distributed phase shifter is shown in figure 4.1. The distributed inductance and capacitance per unit length of the transmission line are represented as L_0 and C_0 , respectively. These values are derived from the intrinsic characteristic impedance Z_0 and phase velocity ν_{ph} of the unloaded transmission line. The tunable shunt capacitance per unit length is represented by C_{var} .

$$Z_0 = \sqrt{\frac{L_0}{C_0}} \quad (4.1)$$

$$\dot{Z}_0 = \sqrt{\frac{L_0}{C_0 + C_{var}}} \quad (4.2)$$

$$\nu_{ph} = \frac{1}{\sqrt{L_0 C_0}} \quad (4.3)$$

$$\nu'_{ph} = \frac{1}{\sqrt{L_0 (C_0 + C_{var})}} \quad (4.4)$$

The relationship between the distributed transmission line parameters and the circuit model elements are given by equations (4.1) and (4.3). These values are functions of the geometry and material properties of the transmission line and cannot be changed. The addition of the tunable shunt capacitance alters the effective characteristic impedance and phase velocity as indicated in (4.2) and (4.4). It can be seen from equation (4.2) that the addition of a C_{var} lowers the characteristic impedance. Therefore it is necessary that the intrinsic characteristic impedance of the transmission line be larger than the characteristic impedance of the external circuit in order to attempt an impedance match. A perfect match is not possible under all tuning conditions, as can be seen from equation (4.2), since C_{var} varies with bias. The variation of phase velocity, as in equation (4.4), is responsible for the phase shifting behavior of the distributed phase shifter.

One crucial design aspect not covered by the previous equations is the periodic nature of the circuit. The discontinuities created by the addition of shunt elements results in small reflections from each element as the signal propagates along the length of the circuit. As the frequency of the signal approaches a certain value, the phases of the incident and reflected signal interfere destructively, preventing forward propagation of the wave. When the signal cannot propagate, the transmission loss increases, and the signal is reflected back towards the source. The frequency where the signal is completely prevented from forward propagation is called the Bragg frequency, after a similar phenomenon in crystalline solids. The relationship between this frequency, f_{Bragg} and the circuit model elements is defined in equation (4.5).

$$f_{Bragg} = \frac{1}{\pi \Delta l \sqrt{L_0(C_0 + C_{var})}} \quad (4.5)$$

The Δl parameter represents the spacing between tuning capacitors, and can be adjusted to change the Bragg frequency independent of the other transmission line parameters. The highest operating frequency of the phase shifter must be significantly below f_{Bragg} to avoid large transmission losses. Modeling the circuit with ABCD matrices will easily demonstrate how transmission loss varies with f_{Bragg} . The phase shift of each section of the distributed phase shifter varies as ν'_{ph} is tuned. The length Δl divided by the change in ν'_{ph} determines the differential phase shift of the section. This is expressed in equation (4.6) with the phase velocity expanded into its constituent terms. The terms C_{min} and C_{max} denote the extremes of the values C_{var} can assume with tuning. A sufficient number of sections should be cascaded to obtain the desired differential phase shift.

$$\Delta\phi = 360^\circ f \Delta l \sqrt{L_0} (\sqrt{C_0 + C_{max}} - \sqrt{C_0 + C_{min}}) \quad (4.6)$$

A loss optimized distributed phase shifter design depends on proper selection of Δl and Z_0 . Increasing Δl brings the Bragg frequency closer to the operating frequency and reduces the number of sections required to achieve a desired phase shift. Increasing Z_0 lowers C_0 and allows a greater variation in ν'_{ph} , and also reducing the number of sections. This is beneficial if the tunable capacitor is lossy, since fewer are needed in a given design. However, operating closer to the Bragg frequency increases the transmission loss through reflection of the input signal. Also, high impedance transmission lines generally have higher loss than lower impedance ones. These conflicting requirements lead to an optimized design that balances the sources of loss, resulting in the lowest loss design. As a result, the best design from a loss

perspective may not necessary have the shortest length or fewest sections.

4.1 Strategies for Size Reduction

As mentioned previously, the principal drawback of the distributed analog phase shifter is its long length. If the number of sections can be decreased or if the individual sections are shortened while maintaining the desired phase shift, the overall phase shifter length can be reduced. Both of these objectives can be achieved by increasing the characteristic impedance of the unloaded transmission line. Increasing Z_0 decreases the distributed capacitance, allowing a larger loading capacitor. The increase in loading capacitor to distributed capacitance ratio increases the phase shift per section. Also, increasing Z_0 increases the distributed inductance, leading to a shorter section length for a given f_{Bragg} .

Coplanar waveguide has been the favored transmission line medium to date for the implementation of distributed phase shifter circuits. The simple connection of shunt elements makes it ideal for connecting a large number of varactors to ground. This is true regardless of the technology used; semiconductor diodes, microelectromechanical membranes, and ferroelectric thin film varactors are all easily integrated into the coplanar waveguide transmission line structure.

Normal use of CPW in MMICs as an interconnect or resonant element requires it to have a characteristic impedance of 50 Ohms. For most substrate materials, this is close to lowest attenuation impedance. When the impedance increases much above this value, the center conductor width narrows rapidly, and high transmission losses are incurred. In [1], an optimization procedure was developed to balance this transmission line loss against the increased varactor diode loss encountered with using lower impedance lines. In [2], quartz substrate material with a dielectric constant of 4 was

used make lower loss high impedance CPW transmission lines. The low dielectric constant widens the center conductor considerably. However, this strategy renders the standard 50Ω line rather lossy for reasonable ground to ground separations, making it a poor choice for integration with other distributed circuit elements. Also, the effective relative dielectric constant of the transmission line decreases to less than 3, further increasing the distributed phase shifter length. In [3], a moderately high transmission line impedance of 70Ω was used, but the ground to ground spacing of the CPW line was increased considerably to widen the center conductor width. The transmission line loss was kept low, but at a considerable expense in chip area. A cross section of the transmission line used there measures nearly half a centimeter in width, enormous by integrated circuit standards.

Two different strategies were pursued here to realize reduced size distributed analog phase shifters. One method is to do away with the transmission line, and implement the inductance with a planar spiral inductor. This technique shrinks each unit cell considerably, but is limited in frequency. The other technique is to utilize the coplanar strip transmission line. This little used transmission line has low loss high impedance lines, making it ideally suited for distributed phase shifters. Both methods present additional challenges and drawbacks, but both are more viable for mass production than the avenues pursued previously.

4.2 Synthetic Transmission Lines

The distributed analog phase shifter is amenable to implementation with the transmission line replaced by a planar spiral inductor. While elimination of the distributed transmission line may make the name seem inappropriate, the principle is the same. Each unit cell of the lumped analog phase shifter consists of a spiral inductor and a shunt varactor. The fixed capacitor to

ground in figure 4.1 is eliminated, except as a parasitic. The structure retains the same wideband frequency characteristics of the distributed version, but is considerably smaller. At frequencies around or below 5 GHz, where distributed elements are unthinkable due to size constraints, the use of spiral inductors makes the distributed analog phase shifter a viable option.

The well known difficulties in closed form modeling of spiral inductors is not as serious a drawback here as in other designs. Since the phase shifter consists of a unit cell repeated many times, only one inductance value is needed. The principal drawback of using spiral inductors is their increased loss compared to transmission lines. Optimization with electromagnetic field solvers can be carried out to find the inductor geometry with the lowest series resistance.

An additional optimization parameter is available here that is not directly applicable in a truly distributed structure. It was previously stated that f_{Bragg} should be set to a frequency sufficiently above the operating frequency to reduce return losses. This frequency must also be kept sufficiently close to the operating frequency to keep the number of sections to a minimum. The total length of the transmission line is identical regardless of the Bragg frequency, making the line attenuation a constant. In most technologies, it is desirable to keep the number of sections low to reduce the cumulative varactor loss.¹ When spiral inductors are used instead of transmission lines, the assumption of constant line loss regardless of Bragg frequency is no longer true. A lower f_{Bragg} design using a smaller number of higher valued inductors may incur more loss than a design using a larger number of smaller inductors. The variation of inductor Q with inductance is complicated, and must be found through electromagnetic simulation. Additional complications result

¹While the individual varactor values vary with changes in the Bragg frequency, it is assumed here that the fixed loss of a varactor is much greater than the value dependent loss variation.



Figure 4.2: An X-band quasi-distributed analog phase shifter.

when inductor Q and varactor Q are similar in magnitude, leading to a complex relationship for the lowest loss design.

As with the previous phase shifter designs presented, the design frequency for this work was 10 GHz. The X-band frequency range, in addition to being of interest for phased array radars, is sufficiently high that distributed techniques are compact enough to be considered for use. This frequency range also begins to test the limits of spiral inductor usage, mainly due to loss considerations, but due to parasitic capacitance and self-resonance.

A synthetic transmission line phase shifter is pictured in 4.2. The three section device was designed to provide 90° of phase shift at 10 GHz. It measured 1.5mm in length, with a total area of 0.75mm^2 . A difference from an earlier device presented in [4] is the removal of the coplanar waveguide launch. In that structure, two varactors were connected in parallel at each inductor node to maintain symmetry. Theoretically, this should half the parasitic varactor resistance and increase Q . Due to the asymmetry in the inductor causing uneven ground voltages, and the extremely small electrode areas, it was believed that a single varactor design would be higher performing. The inductors were 0.8 nH and the maximum varactor capacitance was 0.5 pF. Without any distributed transmission line capacitance, the tuning of the varactors for phase shift greatly impacts the characteristic impedance of

the device. At zero bias, the structure was designed to have a Z_0 of 63Ω , reducing to 47Ω under tuning.

Each inductor consisted of 1.5 turns of $43\mu m$ wide traces, with a turn spacing of $23\mu m$ and an outer diameter of $380\mu m$. The circular topology theoretically has higher Q, but later designs switched to square spirals to reduce EM simulation times. To increase the metal thickness, the air-bridge layer metalization was overlaid partially onto the spiral trace, giving a $2\mu m$ layer of gold. Assuming a conductivity of $2 * 10^7 S/m$, EM simulation indicated a Q of 50.

The varactors were implemented using the BST parallel plate capacitor process. The top plate measured $5.8\mu m$ by $5.8\mu m$, with a ground spacing of $2\mu m$. This was an early design, so it did not take into account the considerable fringing capacitance of the top electrode. The low frequency capacitor Q was approximately 50. While the design assumed a 3:1 capacitance change, only approximately 2:1 was achieved. This limited the maximum phase shift attainable with the device.

The phase shifter managed to achieve 72° differential phase shift with $-1.7dB$ insertion loss at the design frequency of 10 GHz. This resulted in a figure of merit of $42^\circ/dB$. Return loss was kept below $-10dB$. The actual test data are summarized in figures 4.3 and 4.4. This performance is very promising, due to the extremely compact circuit size. A complete 360° design should be achievable in less than $3.0mm^2$ of die area, making it extremely cost competitive to commercial MMIC designs. To make the device performance competitive, the figure of merit should improve to at least $90^\circ/dB$. To achieve this, higher component Qs are necessary. The inductor Q of 50 is quite good, but could be improved upon by copper or silver metalization. The main obstacle at present is the BST varactor loss. Both electrode loss and film loss are significant contributors. Thin, resistive electrode layers are the result

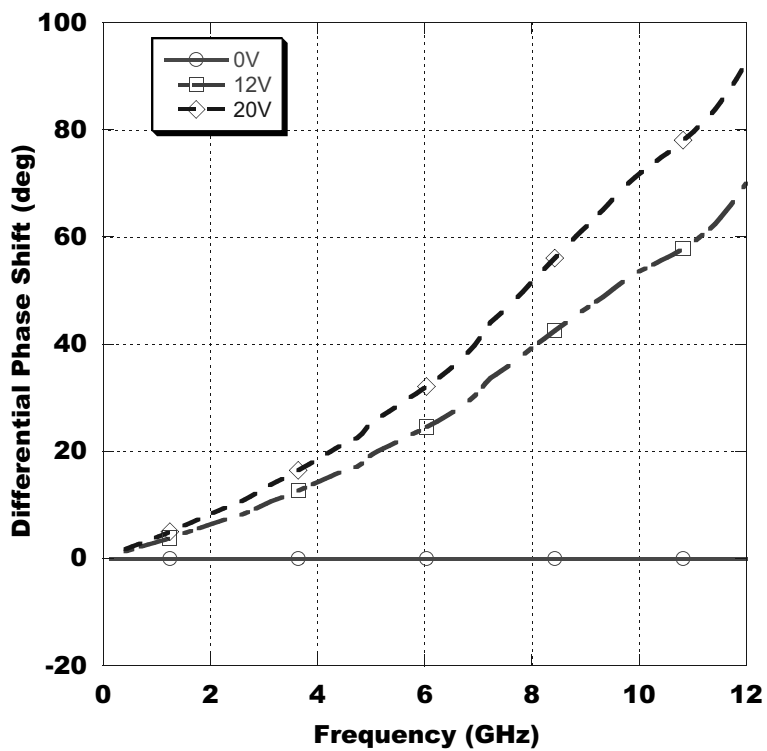


Figure 4.3: Differential phase shifter of 10 GHz lumped device.

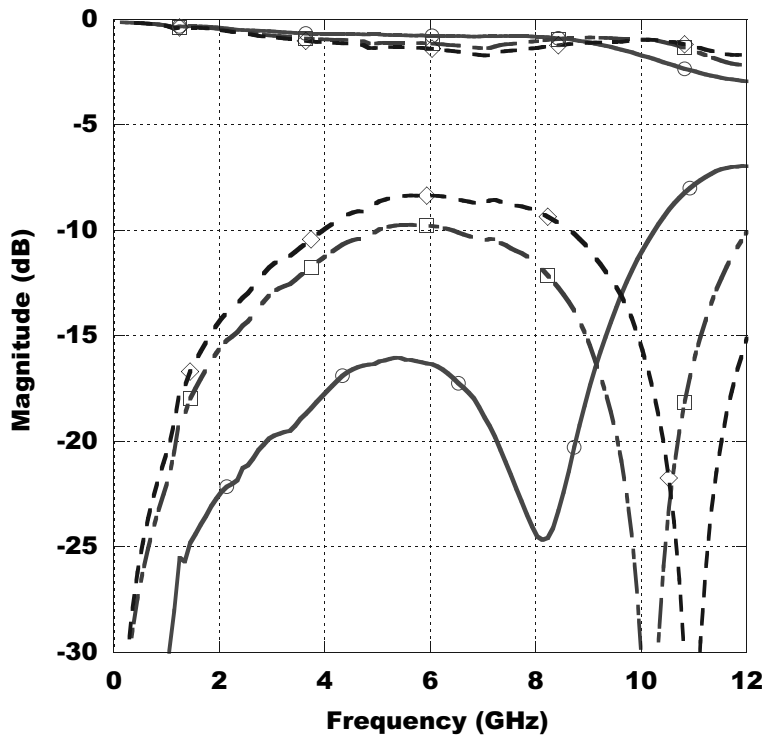


Figure 4.4: Reflection and insertion loss of 10 GHz lumped device.

of high BST growth temperatures and the limitations of contact lithography. Film loss is worsened by long growth times (approximately 3 hours) necessary to increase electrode areas. Most of these issues can be rectified with better process technology.

Attempts were made to improve upon these results with another design iteration. Three devices were designed to provide 180° differential phase shift. These devices varied in mainly in the choice of inductor geometry. However, time constraints only permitted one successful process run. The device figure of merits did not exceed those previously presented. While these designs used square spiral inductors, it is believed the fault lay mainly in poor BST varactor performance.

4.3 High Impedance Coplanar Strip Transmission Lines

The coplanar strip transmission line has seen little use in mainstream microwave circuits. It retains the distinguishing feature of CPW, namely, simple connection of shunt elements. However, one of its primary drawbacks is a rather lossy 50Ω line. The coplanar strip transmission line consists of two parallel conducting strips separated by a gap. At lower impedances, this gap becomes very narrow, and attenuation increases rapidly. As the gap is increased in size (while maintaining a constant conductor width), the impedance increases correspondingly. Formulas given in [5] and [6] are used to plot the loss versus impedance characteristic in figures 4.5 and 4.6. As can be seen from the graphs, the loss rapidly decreases from high levels at lower impedances, and levels out or reaches a minimum near 100Ω . While its loss near 50Ω does not prohibit its use in many microwave circuits, its symmetry characteristics causes it to be a balanced transmission line. This makes the in-line connection of elements such as transistors rather difficult. However,

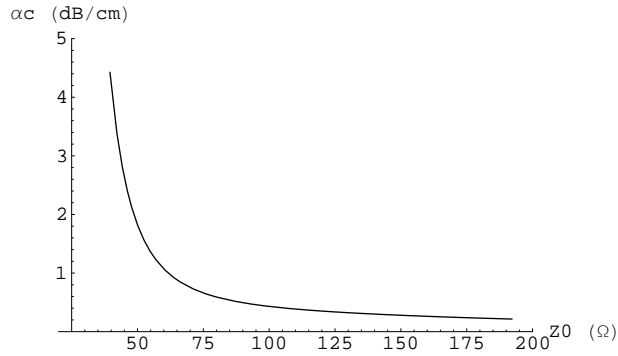


Figure 4.5: Loss versus characteristic impedance plotted with a constant conductor width of $50\mu m$. The substrate has a relative dielectric constant of 10.2, and the metalization is $1\mu m$ of gold.

CPS can easily be integrated with CPW, as demonstrated in [7]. With this in mind, the balanced nature of CPS circuit components can be exploited to effect in carefully designed microwave integrated circuits.

At very high impedances the distributed capacitance of a transmission line becomes almost negligible in comparison to the loading capacitance necessary to reduce its impedance to 50Ω . This makes sections of coplanar strip comprising a distributed phase shifter almost entirely inductive. Unlike a spiral inductor, the coplanar strip segment doesn't have a maximum useful frequency determined by its self-resonant frequency. A distributed transmission line phase shifter can be designed for frequencies much beyond those achievable by synthetic line phase shifters. At frequencies where spiral inductors are still useful, coplanar strip designs can still be used where loss performance is critical, and die area is not as much of a concern. CPS based distributed phase shifters at any frequency are still much more cost-effective than CPW based designs.

Unlike CPW, which becomes lossy at both low and high impedances, CPS's loss continually decreases almost continually with increasing impedance.

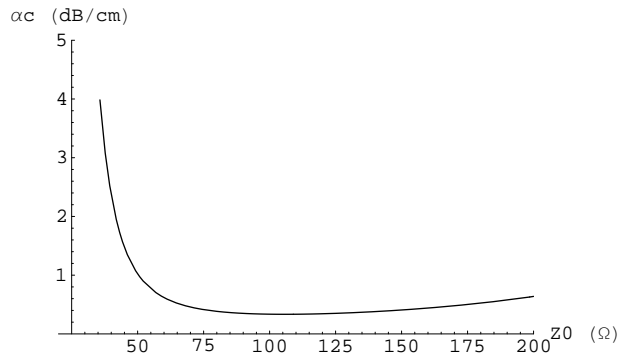


Figure 4.6: Loss versus characteristic impedance plotted while holding the overall transmission line width constant at $200\mu m$, and varying the conductor width and spacing. The material parameters are as before.

The limitation on how high of an impedance can be used is usually based on geometry considerations. As the impedance is raised, the gap between the conductors increases steadily, if the conductor widths are held constant. Eventually, the gap will become comparable in value to the substrate thickness. When this occurs, it will become possible to excite the parasitic microstrip mode at discontinuities. It may also become difficult to excite the line. The CPS gap must therefore be kept below the substrate thickness. Shrinking the conductor widths will decrease the gap size for a given impedance, but will also increase loss.

Another concern with high impedance levels in CPS occurs at high frequencies. The conductor width and gap combination chosen for low loss performance may become comparable to the section length at higher microwave frequencies. This is not recommended because the parasitic inductance of the shunt connection between the two conductors becomes significant compared to the distributed inductance and varactor capacitance of each section. It therefore becomes necessary to shrink the conductor and gap dimensions, increasing transmission line loss.

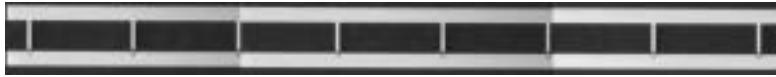


Figure 4.7: A seven section coplanar strip distributed phase shifter.

When transmission lines are loaded with variable capacitance, the effective characteristic impedance varies with tuning. The mismatch to the fixed external circuit impedance is exacerbated with transmission lines of high impedance. A 100Ω CPS transmission line with conductors $65\mu m$ wide and a gap of $70\mu m$ on a $300\mu m$ thick c-plane sapphire substrate has a distributed capacitance of $78pF/m$. The additional shunt capacitance that would bring the effective impedance to 50Ω is $235pF/m$. Assuming a capacitance tuning ratio of 2.5:1, the effective impedance of this line would increase to 67Ω with maximum tuning. With larger tuning ratios or a higher intrinsic Z_0 , the mismatch will increase. To minimize the mismatch, it is beneficial to deliberately mismatch the phase shifter at both extremes of the tuning capacitance range. If the previously described line was instead loaded with $366pF/m$, the effective Z_0 would vary from 42Ω to 59Ω with tuning. This has the additional benefit of increasing the differential phase shift per section slightly while simultaneously providing better input and output matches.

A coplanar strip distributed phase shifter was designed to provide 180° of differential phase shift at 10 GHz. The intrinsic transmission impedance was set at 123Ω , using $75\mu m$ wide conducting strips. It consisted of 7 sections each $990\mu m$ long. Each section was loaded with a BST capacitor measuring $0.5pF$ under zero bias. The characteristic impedance of the phase shifter varied from 40Ω to 70Ω under tuning. The circuit measured $7.3mm$ by $0.3mm$. The fabricated die is pictured in figure 4.7.

The circuit demonstrated a maximum of 120° differential phase shift at 10 GHz. The maximum insertion loss was $-2.6dB$ and the return loss was

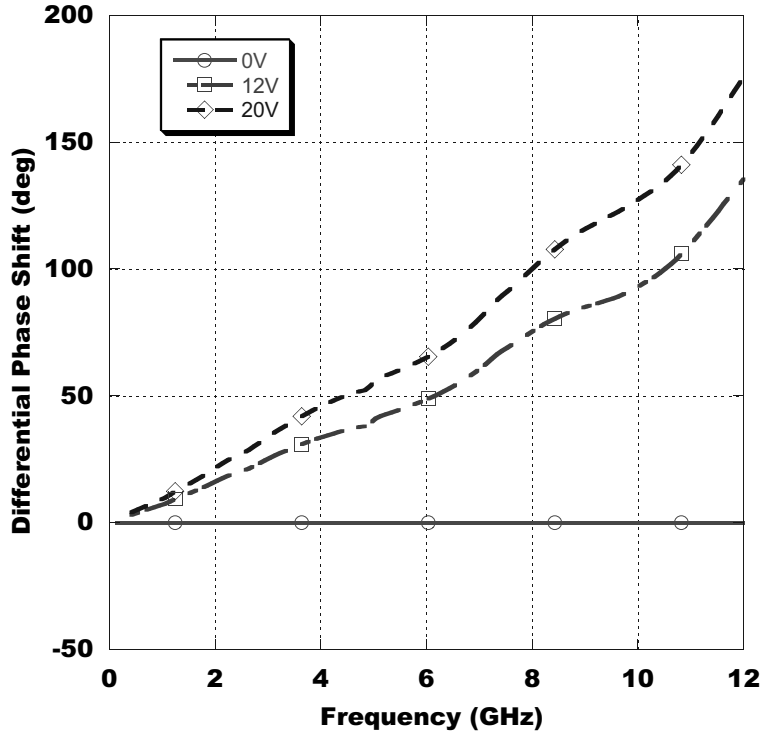


Figure 4.8: Differential phase shift to 12 GHz for the designed coplanar strip phase shifter.

better than $-9dB$ at this frequency. This gives a figure of merit of $49^\circ/dB$ at the design frequency. A full frequency sweep to 12 GHz is given in figures 4.8 and 4.9. The full 180° phase shift range was not achieved for several reasons. The BST capacitance density varied significantly over the wafer. This is not normally seen, and cannot be explained. In addition, a 3:1 tuning ratio was assumed in the design of the circuits. This amount of tuning can be realized if BST with a 50:50 Ba/Sr composition is deposited. At the time of fabrication, only 30:70 material was available. The lower fraction of barium decreases the film leakage, but also decreases the tuning ratio to around 2:1.

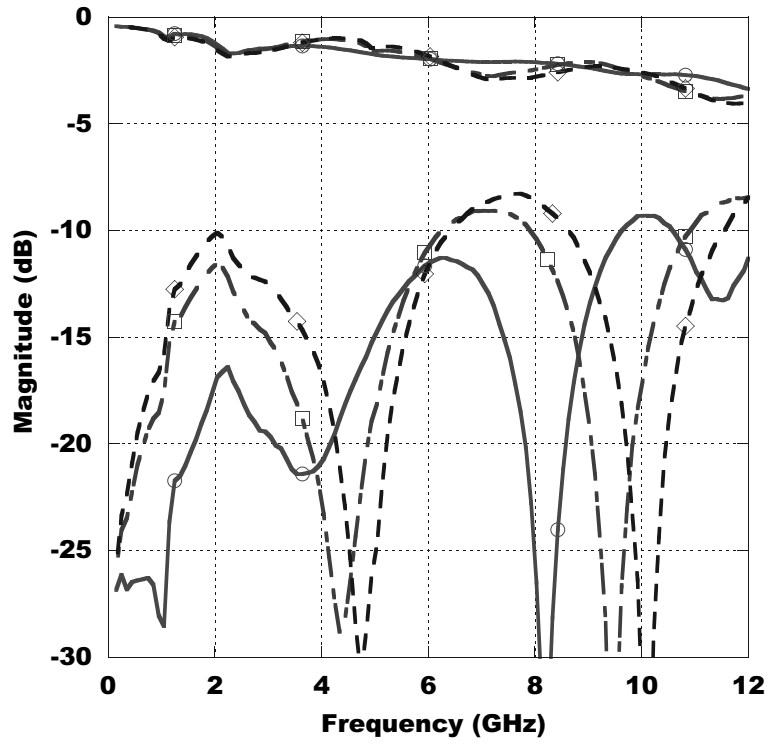


Figure 4.9: Insertion and reflection loss of the design X-band phase shifter.

4.4 Comparisons

The relative dimensions of the two circuits can be compared. If the lumped element design is scaled to a 180° , it will measure 3.0mm . This is less than half the length of the 7.3mm CPS phase shifter. The area consumed by the lumped circuit is a fraction of that occupied by the CPS circuit, which requires a 'buffer' between adjacent lines to mitigate coupling effects. The lumped circuit is not as sensitive to coupling effects. The figure of merit of the lumped version is competitive with the CPS circuit, $42^\circ/dB$ versus $49^\circ/dB$. It is not expected that this trend would continue for higher frequencies. The loss in high frequency spiral inductors is expected to make such lumped phase shifters unfeasible at or above K-band. Data from a CPW distributed phase shifter described in [3] indicates a figure of merit of $80^\circ/dB$. The CPW based circuit offers with best performance in term of loss, but its area is much larger than the other circuits. Measuring 17.5 mm by 3.5 mm , its dimensions ensure wide conductors and a low loss transmission line. It is very inefficient from an area perspective, consuming over half a square centimeter of substrate area. The CPS based circuit consumes only a sixth of the area, but offers superior performance in terms of loss per unit length. The degrees per decibel figure of merit can clearly stand some improvement to make it more comparable to the CPW version. The lumped circuit consumes only one thirtieth the area of the CPW circuit, but still manages to attain reasonable loss performance.

Clearly, when the operating frequencies are low enough, lumped transmission line phase shifters are superior from a cost perspective. The reduced size also offers benefits from an integration standpoint. From the perspective of ultimate loss performance regardless of chip area, the CPW design is still advantageous. Although it not complete obvious from the set of data presented here, we believe the CPS distributed phase shifter has advantages over both

designs. It is possible to scale the CPS circuit to frequencies beyond those feasible with lumped elements, while maintaining a size advantage over CPW circuits. The results are still encouraging. A new type of distributed phase shifter using the coplanar strip transmission line topology was presented that achieved a $49^\circ/dB$ figure of merit. A lumped transmission line circuit was also presented that achieved a $42^\circ/dB$ figure of merit. Both circuits utilized thin film ferroelectric technology and operated at 10 GHz.

Bibliography

- [1] A.S. Nagra and R.A. York, "Distributed Analog Phase Shifters with Low Insertion Loss," *IEEE Trans. Microwave Theory Tech.*, vol.47, no.9, pp. 1705-1711, Sept. 1999
- [2] N.S. Barker and G.M. Rebeiz, "Optimization of Distributed MEMS Transmission-Line Phase Shifters – U-Band and W-Band Designs," *IEEE Trans. Microwave Theory Tech.*, vol.48, no.11, pp. 1957-1966, Nov. 2000
- [3] B. Acikel, T. R. Taylor, P. J. Hansen, J. S. Speck, and R. A. York, "A New High Performance Phase Shifter using BaSrTiO₃ Thin Films," *IEEE Microwave and Wireless Component Letters*, vol.12, no.7, pp. 237-239, July 2002.
- [4] J. Serraiocco, B. Acikel, P. Hansen, T. Taylor, H. Xu, J.S. Speck, and R.A. York, "Tunable Passive Integrated Circuits using BST Thin Films," *Proceedings of the International Symposium on Integrated Ferroelectrics*, Nara, Japan, June 2002
- [5] E. Chen and S.Y. Chou, "Characteristics of Coplanar Transmission Lines on Multilayer Substrates: Modeling and Experiments," *IEEE MTT* June 1997
- [6] G. Ghione, "A CAD-Oriented Analytical Model for the Losses of General Asymmetric Coplanar Lines in Hybrid and Monolithic MICs," *IEEE MTT* Sept. 1993

- [7] M.C. Scardelletti, G.E. Ponchak, and T.M. Weller, "Miniaturized Wilkinson Power Dividers Utilizing Capacitive Loading," *IEEE Microwave and Wireless Components Letters*, vol.12, no.1, pp. 6-8, Jan. 2002

Chapter 5

Conclusion

A number of compact phase shifters using the integrated BST varactor passives process have been presented. The circuits fall into two categories, with either size or performance as their emphasis. The RTPS is a simple design advantageous when smaller amounts of phase shift are needed, while the distributed phase shifter can be scaled up to arbitrarily large phase shifts. These designs can be implemented in almost any technology, but the integrated BST process can potentially be made much cheaper.

Reflection type phase shifters implemented using lumped components have a clear advantage over other designs in terms of die size. An X-band design presented here measured a miniscule 0.36mm^2 in size. To obtain equally impressive loss performance requires careful design entailing extensive electromagnetic simulation, and high quality lumped components. While MIM capacitors and BST varactors can be scaled up in frequency beyond 20 GHz, spiral inductors cannot. This is not a serious hindrance; distributed components can easily be substituted at these frequencies. The RTPS design is however more difficult to scale to large phase shifts than other designs. The tunability ratio places a restriction on the amount of attainable phase shift. This can be extended at lower frequencies by using an integral impedance transformer, which maintains compact circuit size. The design mentioned

previously attained 250° of phase shift with $-10dB$ insertion loss. $25^\circ/dB$ is clearly not competitive enough for commercial use, but with further optimization and improvements in the BST varactor Q , higher figures of merit are possible.

Distributed analog phase shifters have already proven themselves with regard to loss and frequency scalability. Current implementations are excessively large, due to the large number of sections required to achieve the designed phase shift. By transitioning to a coplanar strip transmission line, distributed phase shifters can be realized with higher intrinsic characteristic impedances. This allows heavier loading of the transmission line, resulting in shorter sections with greater amounts of phase shift. This translates into a shorter overall design, consuming less die area, and requiring fewer varactors. A X-band coplanar strip distributed analog phase shifter presented here attained 120° of phase shift while measuring $7.2mm$ in length. An attempt was made to further shrink this design by using spiral inductors instead of a transmission line. One design achieved $42^\circ/dB$ figure of merit. When scaled this design would be less than half the length of the CPS version, while maintaining competitive performance. This technique can be used to extend the performance and true time delay characteristics of the distributed phase shifter to low microwave frequencies.